



The influence of surface materials on microbial biofilm formation in aviation fuel systems

Juan F. Mujica-Alarcon, Jaime Gomez-Bolivar, James Barnes, Myrsini Chronopoulou, Jesus J. Ojeda, Steven F. Thornton & Stephen A. Rolfe

To cite this article: Juan F. Mujica-Alarcon, Jaime Gomez-Bolivar, James Barnes, Myrsini Chronopoulou, Jesus J. Ojeda, Steven F. Thornton & Stephen A. Rolfe (10 Mar 2025): The influence of surface materials on microbial biofilm formation in aviation fuel systems, Biofouling, DOI: [10.1080/08927014.2025.2471366](https://doi.org/10.1080/08927014.2025.2471366)

To link to this article: <https://doi.org/10.1080/08927014.2025.2471366>



© 2025 The Author(s). Published by Informa UK Limited, trading as Taylor & Francis Group



[View supplementary material](#)



Published online: 10 Mar 2025.



[Submit your article to this journal](#)



Article views: 127



[View related articles](#)



[View Crossmark data](#)

The influence of surface materials on microbial biofilm formation in aviation fuel systems

Juan F. Mujica-Alarcon^a, Jaime Gomez-Bolivar^a, James Barnes^b, Myrsini Chronopoulou^c, Jesus J. Ojeda^d, Steven F. Thornton^e and Stephen A. Rolfe^a

^aSchool of Biosciences, University of Sheffield, Sheffield, UK; ^bAirbus Operations Ltd, Pegasus House, Bristol, UK; ^cConidia Bioscience Ltd, Unit 6 Surrey Technology Centre, Guildford, Surrey, UK; ^dDepartment of Chemical Engineering, School of Engineering and Applied Sciences, Swansea University, Swansea, UK; ^eGroundwater Protection and Restoration Group, School of Mechanical, Aerospace and Civil Engineering, University of Sheffield, Sheffield, UK

ABSTRACT

The ability of different microbes to form biofilms on materials found in aviation fuel systems was assessed using both individual isolates and complex microbial communities. Biofilm formation by the Gram-negative bacterium, *Pseudomonas putida*, the fungus *Amorphotheca resiniae* and the yeast, *Candida tropicalis*, was influenced by material surface properties although this differed between isolates. Biofilm formation was greatest at the fuel–water interface. The Gram-positive bacterium *Rhodococcus erythropolis*, in contrast, was able to grow on most surfaces. When a subset of materials was exposed to complex microbial communities, the attached microbial community structure was influenced by surface properties and selected for different genera best able to form biofilms on a specific surface. Distinct sub-populations of *Pseudomonads* were identified, which favoured growth on aluminium or painted surfaces, with a different subpopulation favouring growth on nitrile.

ARTICLE HISTORY

Received 22 July 2024
Accepted 18 February 2025

KEYWORDS

Biofilms; fuel contamination; aviation; surface properties

Introduction

Microbial contamination of fuel systems is a major problem faced by the aviation industry, the prevention, control, and mitigation of which requires significant economic investment. Contamination must be routinely tested for, and significant contamination requires aircraft to be withdrawn from service for decontamination. Microbial activities can cause fuel deterioration, microbially-influenced corrosion (MIC) and biofouling of surfaces, sensors and filters (Gaylarde et al. 1999, Passman 2013, Smith 1991). In aircraft fuel systems, fuel degradation is generally limited (unless aircraft are stored for extended periods) as fuel is constantly used and replenished. However, during aircraft operations, water condenses within the fuel tanks creating an aqueous environment and a fuel–water interface (Chan and Lam 2017). This provides an environment in which microbes can grow, either in suspension (planktonic) or attached to surfaces (as biofilms). Microbes can even grow in the fuel phase in entrapped water droplets (Meckenstock et al. 2014). Microbes in the liquid

phases are lost as fuel is consumed and water removed by scavenging systems or drainage. However, communities attached to surfaces will persist as biofilms, developing over extended periods, and acting as an inoculum for replenished liquid phases.

The influence of surface materials used in aircraft fuel systems on the formation of microbial biofilms is not well understood. Diverse bacteria and fungi have been reported as fuel system contaminants (e.g. Gaylarde et al. 1999, Hu et al. 2020, Passman 2013, Rauch et al. 2006, White et al. 2011). A recent analysis of over 1,200 swabs and liquid samples from aviation fuel systems showed that α -, β -, and γ -Proteobacteria and Ascomycota (particularly the filamentous fungus, *Amorphotheca resiniae*, synonyms *Cladosporium* or *Hormoconis resiniae*) were prevalent in contaminated systems (Krohn et al. 2021), although the community composition of different samples varied greatly. Metagenomic and transcriptomic analysis highlighted the importance of genes associated with biofilm formation and alkane degradation. Some

CONTACT Stephen A. Rolfe  s.rolfe@sheffield.ac.uk

 Supplemental data for this article can be accessed online at <https://doi.org/10.1080/08927014.2025.2471366>

© 2025 The Author(s). Published by Informa UK Limited, trading as Taylor & Francis Group
This is an Open Access article distributed under the terms of the Creative Commons Attribution License (<http://creativecommons.org/licenses/by/4.0/>), which permits unrestricted use, distribution, and reproduction in any medium, provided the original work is properly cited. The terms on which this article has been published allow the posting of the Accepted Manuscript in a repository by the author(s) or with their consent.

prominent community members were identified as difficult to culture. Shapiro et al. (2021) also found bacteria associated with fungi in aviation fuel systems that they were unable to isolate and which they proposed formed synergistic systems for kerosene degradation. Therefore, understanding the factors that control biofilm formation in aviation fuel systems must account for their compositional complexity and interactions between community members.

Aircraft fuel systems are composed of diverse materials including aluminium alloys, stainless steels, paints and sealants, rubbers and plastics, providing a multitude of surfaces for biofilm formation. Surfaces have different physico-chemical properties (e.g. hydrophobicity, surface roughness, charge and chemistry) and are exposed to hydrophobic fuels and hydrophilic aqueous phases. A number of studies have explored the impact of microbes on surfaces. A community dominated by *Bacillus* sp. caused biocorrosion of aluminium AA2024 coupons (McNamara et al. 2005) and a *Bacillus* strain corroded aluminium AA2024 and AA707512 (Vejar et al. 2017). Likewise, *B. cereus* ACE4 and *Serratia marsescens* ACE2 corroded AA2024 (Rajasekar and Ting 2010). Numerous bacterial and fungal isolates were able to corrode AA7075 (Hagenauer et al. 1994).

A systematic analysis of biofilm formation on the materials found in aviation fuel systems has not been undertaken but has the potential to identify surfaces that might limit biofilm formation, or be particularly susceptible to biofouling, requiring special attention during cleaning. As new materials, such as composites, are used in aircraft construction, understanding their influence on biofilm formation will also help to inform future testing and cleaning regimes for microbial contamination.

The role of material properties on attached microbial growth in medical, food and natural environments has been studied extensively, identifying surface charge, energy and chemistry, hydrophobicity, roughness and stiffness as factors influencing microbial attachment and biofilm maturation (Banerjee et al. 2011, Berne et al. 2018, Song et al. 2015). However, microbial diversity means it has not been possible to develop general models of surface properties that govern microbial attachment. For example, although surface roughness affects microbial attachment, responses differ between cells depending on their size, shape and surface chemistry, with no single topography providing a universal limitation to biofilm formation (Renner and Weibel 2011). This complexity arises, in part, from the biological components of the system, with biofilm formation governed by cell-

surface and cell-cell interactions, and extracellular polymeric substances (EPS) (e.g. polysaccharides, proteins, lipids and nucleic acid) (Flemming and Wingender 2010). The physico-chemical properties of microbes also differ. Gram-negative bacteria have a thin peptidoglycan wall surrounded by an outer membrane containing lipopolysaccharides while Gram-positive bacteria lack this outer membrane, but have a much thicker peptidoglycan layer rich in teichoic acid (Silhavy et al. 2010). Fungal cell walls are also diverse (Gow et al. 2017), consisting of an inner cell wall of branched glucans and chitin surrounded by a highly diverse, glycoprotein rich layer.

To explore the propensity for biofilm formation on materials found in current, or new, aviation fuel systems, an axenic microcosm system was developed where material coupons were incubated with aqueous growth medium overlaid with fuel and inoculated with isolates of common fuel-system microbial contaminants. Biofilm formation was quantified on different materials in the aqueous and fuel phases and at the fuel-water interface. A ranking of materials by biofilm formation was produced and related to material surface properties (hydrophobicity, surface charge and roughness). Microbes that are common contaminants in aviation systems, known fuel degraders and in different taxonomic groups were tested (Denaro et al. 2005, Gaylarde et al. 1999, Itah et al. 2009, Krohn et al. 2021): *Pseudomonas putida* (Gram-negative bacterium), *Rhodococcus erythropolis* (Gram-positive bacterium), *Candida tropicalis* (yeast) and *Amorphotheca resinae* (filamentous fungus).

A subset of these materials was then placed in microcosms containing complex microbial communities originating from a contaminated aviation fuel tank, transferring the coupons at intervals into a new sterile fuel-water mixture, thereby selecting biofilm-forming community members. This system simulated the consumption, and resupply, of fuel in aircraft fuel tanks, testing the hypothesis that repeated removal of the liquid phases would select taxa that were able to attach efficiently to different surfaces.

These approaches were used to address the following questions.

- Which materials found in aviation fuel systems are most prone to biofilm formation by common fuel contaminants? Are there materials which limit biofilm formation?
- Do microbes behave similarly, or are there species-specific differences in biofilm formation on different materials, and in the aqueous and fuel phases?

- Is it possible to identify material properties that influence biofilm formation?
- How do findings from isolated organisms compare to the behaviour of complex communities?

Methods

Materials

The materials used in this study are shown in Table 1.

Coupons were supplied by Airbus and are commercially available materials used in the manufacture of aircraft fuel systems.

Fuel was prepared by filtering 1 l of Merox-treated Jet A-1 through 300 g attapulgitic clay (Fuller's Earth) to remove additives, then 24 mg l⁻¹ 2,6-ditertiary-butyl-phenol (Aldrich Chemistry, USA) added as anti-oxidant, before filter sterilisation through a 0.22 µm nitrocellulose filter (Whatman, Maidstone, Kent, UK).

Individual microbes were obtained from the ATCC stock centre: *Pseudomonas putida* (ATCC 700007), *Rhodococcus erythropolis* (NCIMB 12631), *Amorphotheca resinae* (ATCC 20495), *Candida tropicalis* (ATCC 48138). Bacteria were grown in LB medium (10 g l⁻¹ peptone, 5 g l⁻¹ yeast extract, 10 g l⁻¹ NaCl, Acumedia Lab, Neogen, Lansing, MI, USA) whilst the yeast and fungi were grown in yeast-malt media (3 g l⁻¹ yeast extract, 3 g l⁻¹ malt extract, 5 g l⁻¹ mycological peptone and 10 g l⁻¹ dextrose, LabM, Gentaur UK Ltd, Potters Bar, UK and Sigma-Aldrich, Merck Life Science, Gillingham, UK). Cells were centrifuged at 699 × g for 1 min then resuspended at an OD₆₀₀ of 0.05 in 1/4-strength Bushnell-Haas (BH) medium (0.05 g l⁻¹ MgSO₄, 0.005 g l⁻¹ CaCl₂, 0.25 g l⁻¹ KH₂PO₄, 0.25 g l⁻¹ K₂HPO₄, 0.25 g l⁻¹ NH₄NO₃, 0.0125 g l⁻¹ FeCl₂, pH 6.72; Sigma-Aldrich, UK) as an inoculum.

A complex, mixed community of microbes was established in the laboratory using bottom water from a contaminated fuel tank as an inoculum. The

community was maintained in 500 ml glass bottles (Duran, Fisher Scientific UK Ltd, Loughborough, UK) containing 100 ml 1/4-strength BH medium and 100 ml Merox-treated Jet A-1 aviation fuel. Air exchange was provided by a 0.22 µm PTFE filter in the lid. The community was sub-cultured every month by transferring 5 ml of the aqueous phase into a new system.

Measurement of surface properties

Hydrophobicity was determined using a drop shape analyser DSA100 (Krüss, Hamburg, Germany). A 5 µl droplet of UHQ water was placed on each coupon with a microsyringe, and the contact angle between the droplet and the surface measured. At least five measurements were made for each side of the coupon.

The pH of zero point charge (pHzpc) and charge potential curves were determined by potentiometric titrations (Metrohm 906 Titrando) of 10 × 10 × 2 mm portions of coupons. The material was suspended in 25 ml CO₂ – free electrolyte (0.05, 0.1 or 1.0 M NaCl) and titrated to pH 3.0 with 0.05 M HCl and then pH 11.0 with 0.05 M NaOH. Titration data was analysed with Protokit (version 2.1 rev1) (Turner and Fein 2006). The intersection of the titration curves at different ionic strengths provided the pHzpc. The surface charge at the microcosm pH (sigma, σ) was calculated from the 0.05 M titration curves.

Surface roughness was determined using a Bruker Contour Elite K 3D optical microscope (Bruker Billerica, MA, USA). Measurements of Sa, the arithmetic mean of the absolute differences in peak height, were made at two scales: 636 × 476 µm and 29 × 21 µm. Since the optical profiler relies on reflectance from the materials, dark materials were gold coated before analysis by sputter coating under vacuum using an Edwards S150B Sputter Coater (Edwards Vacuum, Burgess Hill, England) for 2 min at 1 kV and ~20 mA current. Comparisons of gold-coated and uncoated surfaces showed that coating

Table 1. Materials used in this study.

Material	Notes
AA7075 T6	Aluminium 7075 T6 (zinc alloy)
AA2024 T3	Aluminium 2024 T3 (copper alloy)
AA2024 TSA	Aluminium 2024 T3 (copper alloy) anodised
SS304 smooth	Stainless steel 304 – polished surface finish
SS304 rough	Stainless steel 304 – rough surface finish
Primer P60A	P60A water-based primer (chromated) on aluminium MAPAERO
HS37092	HS37092 solvent-based fuel tank coating (chromated) AKZO NOBEL
Topcoat 311_380	Polyurethane surface coating (AERODUR HS 67348)
Composite smooth	Composite – resin transfer moulded
Composite rough	Composite – peel fly manufactured
Sealant MC238	Polysulphide polymer sealant (pure elastomer – AIMS04-05-002)
Sealant MC780	Polysulphide polymer sealant (elastomer and hollow sphere – AIMS 04-05-015)
Elastomer nitrile	Nitrile elastomer ABR 4-0101:55
Elastomer fluorosilicone	Fluorosilicone elastomer ABR 4-0090: 55
Plastic PEI	Polyetherimide plastic PEI 450 G

did not significantly affect surface roughness. The significant differences in surface topology precluded the use of atomic force microscopy.

Microcosm preparation and sampling

Microcosms (prepared in triplicate) consisted of a 20 ml glass vial (Thermo Scientific, Warsaw, Poland) closed with a crimp seal and a PTFE/butyl septum (Agilent, Lexington, MA, USA), a material coupon (dimensions: $63 \times 10 \times 1$ mm), 7 ml of $1/4$ -strength BH medium and 7 ml of fuel. The microcosms were inoculated so that the aqueous phase had a starting OD_{600} of 0.05 and then incubated for four weeks at 25°C . Abiotic controls contained sterile $1/4$ -strength BH medium and fuel. After incubation, coupons were air dried in a sterile environment for 15–30 min to allow fuel vapour to evaporate then fixed in 10 ml of 4% (v/v) formaldehyde (Merck, Germany) and stored at 4°C for cell counts. Counts were completed within four weeks.

Biofilm coverage

Coupons were washed with filter-sterilised 0.15 M NaCl prior to staining. Because some microbial stains interacted with the surface or the material exhibited high autofluorescence, different fluorescent dyes were used, but all stained individual cells. Aluminium alloys and stainless steel coupons were stained with 1 ml of 1:800 diluted SYTO9 ($\lambda_{\text{ex}} = 470$ nm, $\lambda_{\text{em}} = 510$ nm, ThermoFisher Scientific, Altrincham, UK). Primer P60A, fluorosilicone elastomer and MC238 sealant were stained with 1 ml of 1:800 diluted propidium iodide ($\lambda_{\text{ex}} = 535$ nm, $\lambda_{\text{em}} = 617$ nm, Invitrogen eBioscience, Hatfield, UK). The remaining materials were stained with 1 ml of $50 \mu\text{g ml}^{-1}$ acridine orange ($\lambda_{\text{ex}} = 470$ nm, $\lambda_{\text{em}} = 510$ nm, Sigma Aldrich, UK). In each case coupons were stained for 15 min.

Cells were visualised using a DM6 Epifluorescence microscope (Leica, Wetzlar, Germany), an automated stage and a monochrome digital camera (Leica DMC 4500). Images were taken in a grid across the coupon surface to avoid bias in the regions measured. The location of the fuel–water interface was located manually and 3 images of the interface taken 4 mm apart (Supplementary Figure 1a). Additional sets of three images were taken 5 and 10 mm away from the interface into the fuel phase and aqueous phase producing 15 images per coupon. As the coupons were not optically flat, a Z-series of images was obtained at each location and a composite image based on maximum brightness created using Fiji (Schindelin et al. 2012). The percentage coverage was

calculated based on pixels above the background signal. The biofilms produced were not thick due to the low nutrient content of the microcosms (Gómez-Bolívar et al. 2024), hence surface coverage provided a sufficient proxy for microbial growth.

Molecular analysis of complex microbial communities

DNA extraction

The planktonic community used to inoculate the microcosms was sampled by filtration through a $0.22 \mu\text{m}$ nitrocellulose filter (Whatman). Attached communities were sampled by swabbing the coupon surface (Tech Service Consultants Ltd, Heywood, UK) from the aqueous and fuel phases separately. Samples were stored at -80°C prior to DNA extraction. To each swab or filter $720 \mu\text{l}$ of SET buffer (0.75 M sucrose, 40 mM EDTA, 50 mM Tris-Cl pH 9) and $81 \mu\text{l}$ of 10 mg ml^{-1} lysozyme (Sigma Aldrich, UK) were added and vortexed for 10 s. The extraction tubes were vortexed horizontally (Mo bio Laboratories, Carlsbad, CA, USA) at maximum speed for 30 min at 37°C . Then $90 \mu\text{l}$ of 10% (v/v) sodium dodecyl sulphate (SDS) (Sigma-Aldrich, UK), and $25 \mu\text{l}$ of 20 mg ml^{-1} proteinase K (Invitrogen) was added and the tubes incubated at 55°C for 2 h. The supernatant was transferred to a new 2 ml microcentrifuge tube and $137 \mu\text{l}$ 5 M NaCl (Fisher Chemical, Loughborough, UK), $115 \mu\text{l}$ hexadecylmethyl ammonium bromide (CTAB), and $8 \mu\text{l}$ 20 mg ml^{-1} glycogen (Omega Bioservices, Norcross, GA, USA) added. Samples were vortexed for 10 s, incubated at 65°C for 1 h, then $838 \mu\text{l}$ of chloroform added. Samples were vortexed for 10 s and centrifuged at $19,283 \times g$ for 5 min. The upper aqueous layer was recovered and the chloroform extraction repeated. DNA was precipitated by adding $815 \mu\text{l}$ isopropyl alcohol, vortexing for 10 s, incubation overnight at -20°C and centrifugation at $19,283 \times g$ for 30 min. The supernatant was discarded and the pellet washed twice with 1 ml of 70% (v/v) ethanol with centrifugation at $19,283 \times g$ for 10 min. The ethanol was removed and the sample air dried, then resuspended in $50 \mu\text{l}$ of nuclease-free water.

PCR reactions

For sequencing, bacterial 16S rRNA genes were amplified with primers targeting the V3 and V4 region (Klindworth et al. 2013) with Illumina extensions.

These are Illumina-341 F5'-TCGTCGGCAGCGTC AGATGTGTATAAGAGACAGCCTACGGGNGGCW GCAG-3' and Illumina-805 R5'-GTCTCGTGGGCTC GGAGATGTGTATAAGAGACAGGACTACHVGGG-TATCTAATCC-3' Eukaryotic ITS regions (White

et al. 1990) were amplified with Illumina-ITS3F 5'-TCGTCGGCAGCGTCAGATGTGTATAAGAGACAG GCATCGATGAAGAACGCAGC-3' and Illumina-ITS4 R 5'-GTCTCGTGGGCTCGGAGATGTGTATAAGAG ACAGTCTCCGCTTATTGATATGC-3'.

First round PCR reactions contained 2.5 µl of template (5 ng µl⁻¹), 12.5 µl of 2× KAPA HiFi Hot Start Ready Mix (Sigma-Aldrich, UK) and 5 µl of forward and reverse primers. PCR reactions were performed separately for bacterial and fungal primer pairs. The first round PCR conditions were 95 °C for 3 min, 25 cycles of 95 °C for 30 s, 55 °C for 30 s, and 72 °C for 30 s and then a final step of 72 °C for 5 min. Second round PCR reactions contained 10 µl of template, 25 µl of 2× KAPA HiFi Hot Start Ready Mix (Sigma-Aldrich, UK) and 5 µl of forward and reverse Nextera XT Index primers (Illumina, Cambridge, UK). The index PCR conditions were 95 °C for 3 min, eight cycles of 95 °C for 30 s, 55.0 °C for 30 s, and 72 °C for 30 s, and then a final step of 72 °C for 5 min. Amplicons were visualised on 2% (w/v) agarose gels. Sample preparation and sequencing was performed by the Sheffield Diagnostic and Genetics Service (Sheffield, UK) using an Illumina MiSeq instrument, with V2 chemistry flow cell producing 250 bp paired end reads.

Bacterial 16S rRNA and eukaryotic ITS genes were quantified in samples using quantitative, real-time PCR (qRT-PCR). Purified *E. coli* or *C. tropicalis* DNA was used as standards. The 16S rRNA gene was amplified with primers 799 F (5'-AACMGGATTA GATACCCKG-3') and 1193 R (5'-ACGTCATCCC CACCTTCC-3') and eukaryotic ITS genes were amplified with primers ITS3 F (5'-GCATCGATGA AGAACGCAGC-3') and ITS4 R (5'-TCCTCCG CTTATTGATATGC-3'). Results are expressed as copy numbers, assuming the *E. coli* genome contained seven 16S rRNA copies and the *C. tropicalis* genome contained three ITS copies. The reaction mixture contained 1 µl of input DNA, 5 µl of SensiFast™ SYBR® No-ROX Kit (Bioline) mixed buffer and dNTPs, 0.4 µl of each primer (10 µM) and 3.2 µl of nuclease-free water. Amplification was performed using a real-time PCR Thermocycler (Corbett Research RG-6000, Qiagen Roto-Gene Q, Qiagen, Manchester, UK) using the following conditions: 95 °C for 3 min followed by 40 cycles of 95 °C for 3 min, 62 °C for 10 s, 72 °C for 10 s with a final melting curve performed over the temperature range 61 °C to 95 °C.

Bioinformatic analysis

Demultiplexed sequences were provided as Fastq files with amplification primers and barcodes removed.

Data were processed using dada2 (Callahan et al. 2016) version 1.18 and the analysis pipelines provided by the authors. For the 16S rRNA sequences, pairs were quality filtered (trunQ = 2, maxEE = 2), error rates calculated and applied, then the pairs merged. Chimeric sequences were removed using the consensus method, with the minFoldParentOverAbundance parameter set to 8 with sequences over 430 bp retained. ITS sequences were analysed in the same way except sequences were concatenated during the merging step. Taxonomies were assigned using the SILVA non-redundant 16S rRNA dataset (99% version 138.1) and the UNITE ITS database (version 8.2) (Abarenkov et al. 2020). An optimised neighbour-joining phylogenetic tree of 16S rRNA sequences was created using the 'phangorn' R package v 2.5.5 (Schliep et al. 2017). ITS sequences are not phylogenetically informative, so no tree was created for fungi. Phylogenetic trees of selected organisms were created using MEGA X (Kumar et al. 2018) and the maximum likelihood method (Tamura and Nei 1993). Differences between community composition on different materials were calculated using DESeq2 (Love et al. 2014). All subsequent bioinformatic analyses were performed in R (R Core Team 2021).

Statistical analysis

All additional statistical analyses were performed in R (R Core Team 2021). Statistical differences in biofilm coverage were determined using the 'betareg' package for beta regression (Cribari-Neto and Zeileis 2010) as values are bounded between 0 and 100%. A small value (0.001%) was added to individual measurements to avoid zero values. Contrasts were compared using the package 'emmeans' (Lenth 2025) with compact letter displays calculated using the package 'multcomp' (Hothorn et al. 2008). Random forests were implemented using the package 'randomForest' (Liaw and Wiener 2002).

Results

The influence of surface material on biofilm formation

Replicate axenic microcosms, containing different coupons of materials found in aviation fuel systems and equal volumes of aqueous growth medium overlaid with jet fuel, were inoculated with either *P. putida*, *R. erythropolis*, *C. tropicalis* or *A. resiniae*. After four weeks of growth the percentage of the coupon surface covered by a biofilm in the fuel phase,

aqueous phase or at the interface was measured using epifluorescence microscopy (Figure 1).

For all isolates, biofilm coverage was greater in the aqueous phase and at the aqueous–fuel interface, than in the fuel phase, due to the more amenable conditions for microbial growth (Figure 1). Coverage in the aqueous phase was correlated significantly with coverage at the interface (Figure 2a). For *P. putida*, and to a lesser extent *A. resiniae*, coverage in these phases

was also correlated significantly with that in the fuel phase. However, for *R. erythropolis* and *C. tropicalis*, there was little or no correlation between coverage in the aqueous phase and at the interface and coverage in the fuel phase.

There were marked differences in coverage on the different materials tested (Figure 1). For example, *P. putida* formed extensive biofilms on aluminium AA7075-T6 but less so on aluminium AA-2024-T3 or AA-20234-

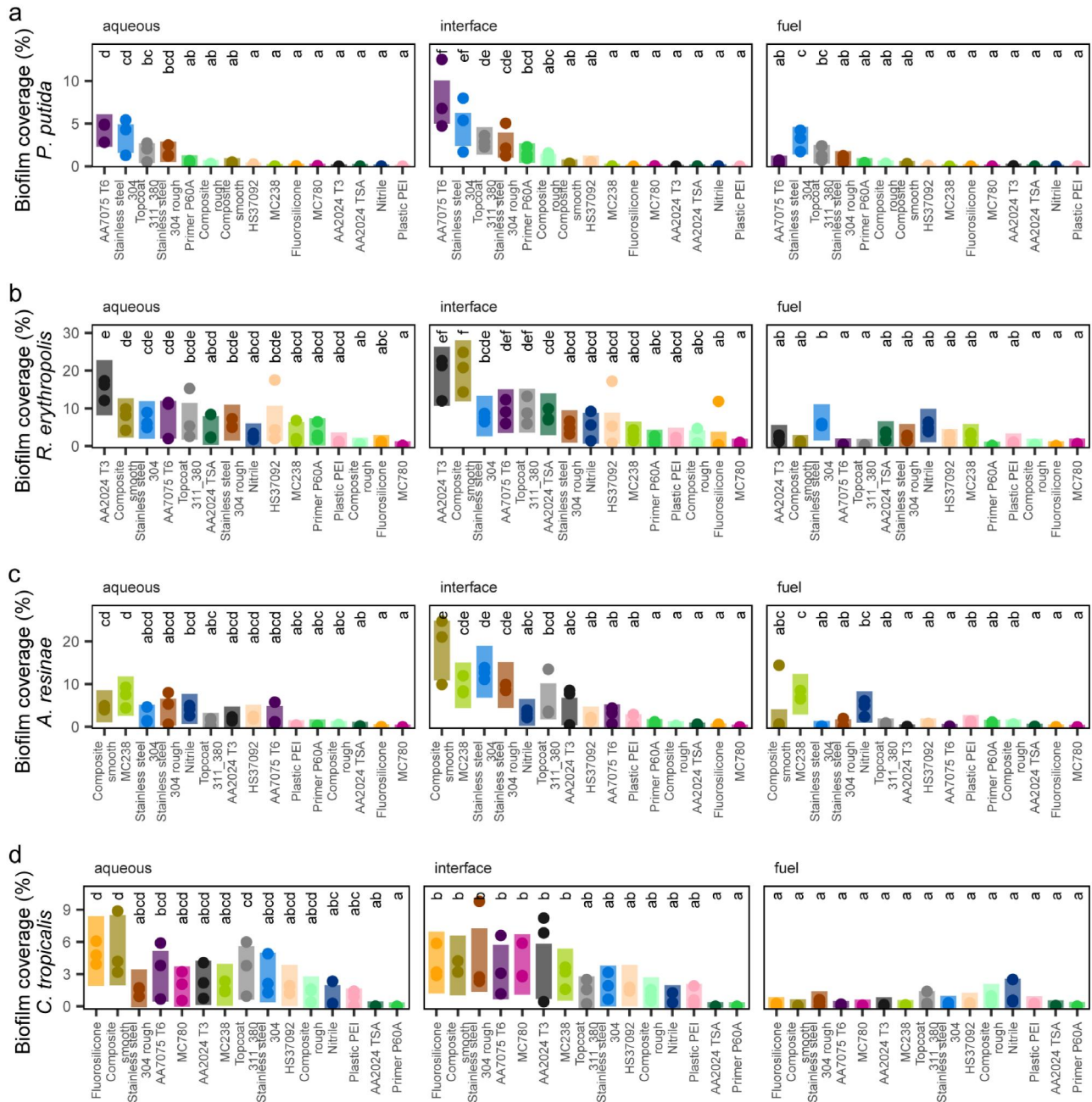


Figure 1. Biofilm coverage by different isolates after four weeks of growth on different coupons. Data points are the mean coverage of all images for a replicate material coupon in the aqueous phase, at the fuel–aqueous interface and in the fuel phase. The bars show the confidence intervals calculated by beta regression with a logistic link function for all replicates ($n = 3$). Bars that share a letter do not differ significantly within a phase. Bars are coloured by material and are ranked by biofilm coverage across all phases for each isolate.

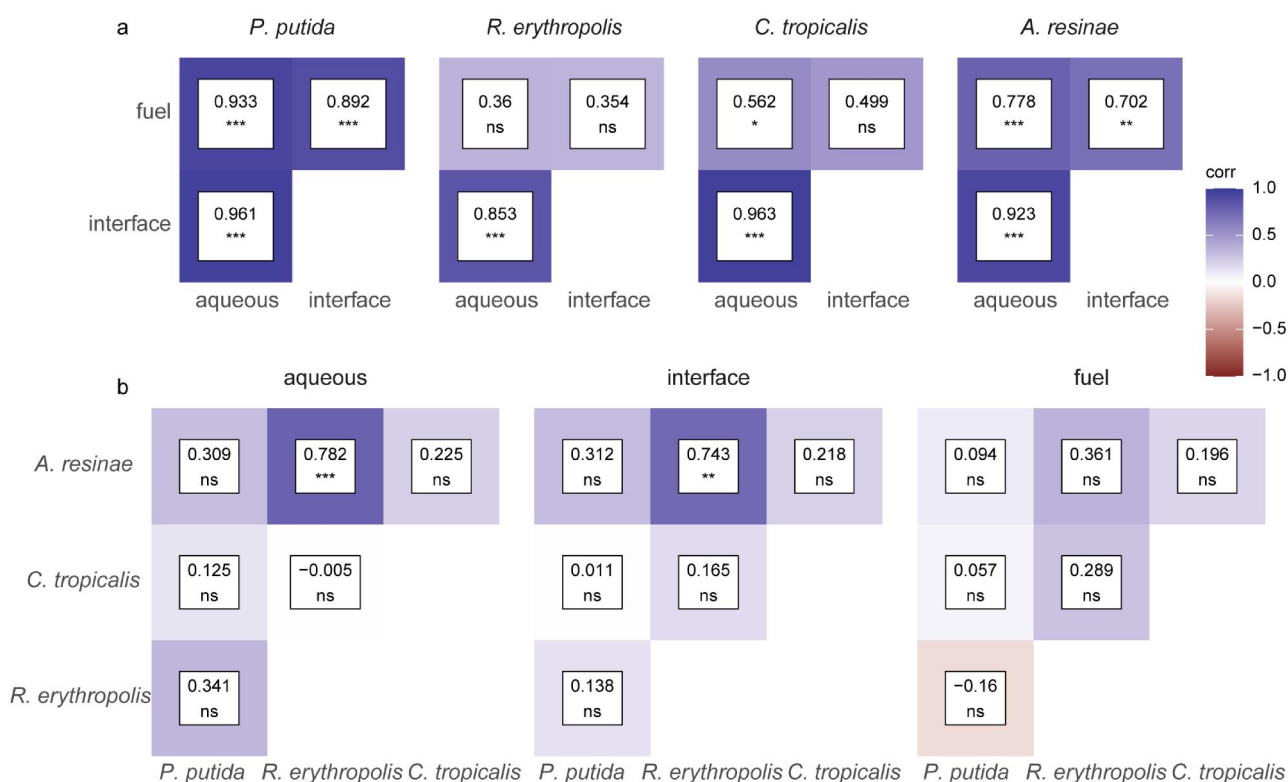


Figure 2. Correlation coefficients of biofilm coverage (a) for each isolate in the aqueous, interface and fuel phases for all materials and (b) between isolates in each phase for all materials. Results are presented as the correlation coefficients and significance (***) $p < 0.001$, (**) $p < 0.01$, (*) $p < 0.05$, ns not significant). Coverage values were log transformed before the Pearson correlation coefficient was calculated.

TSA. In contrast, the coverage of *R. erythropolis* biofilms was similar on all three aluminium surfaces. *C. tropicalis* formed extensive biofilms in the aqueous phase on fluoro-silicone unlike the other isolates tested, where little biofilm formation was observed.

These marked differences in behaviour of the isolates in the different phases are illustrated in Figure 2b. Correlation coefficients calculated for coverage on different materials in each phase were not significant for most comparisons, with the exception of *A. resiniae* and *R. erythropolis* in the aqueous and fuel phases. Overall, no simple pattern of biofilm coverage by the isolates on different materials and different phases was evident.

To determine the overall propensity of biofilms to form on a surface, coverage on each material was ranked for each phase, which accounts for differences in growth rates between organisms. Figure 3 shows the ranked coverage in the aqueous phase plotted against ranked coverage at the interface and in the fuel phase, averaged for the four isolates.

The ranking between the aqueous and interface was closely correlated, with coverage greatest on Stainless steel (smooth and rough), Topcoat 311_380, Composite (smooth) and Aluminium AA7075 T6 and

least on Plastic PEI, Aluminium AA2024 TSA and MC780. Comparisons between the aqueous phase and the fuel phase were more complex. Whilst coverage was ranked similarly for most materials, there was a greater propensity for biofilms to form in the fuel phase with Plastic PEI, Composite (rough) and nitrile. In contrast biofilms formed preferentially in the aqueous phase on Composite (smooth) and Aluminium AA7075 T6.

The impact of surface properties on biofilm coverage by isolated microbes

The surface properties of the materials used in this study are shown in Table 2.

Hydrophobicity was determined by drop shape analysis. The surface roughness was determined by optical interferometry at two scales – the larger scale ($636 \times 476 \mu\text{m}$) related to gross changes in roughness whilst the smaller scale ($29 \times 21 \mu\text{m}$) was chosen as roughness at the level of individual cells. The parameter Sa (arithmetic mean height) was determined. Surface topography maps of these materials are shown in Supplementary Figure 2. Acid/base titration at different ionic strengths was used to calculate the pH of

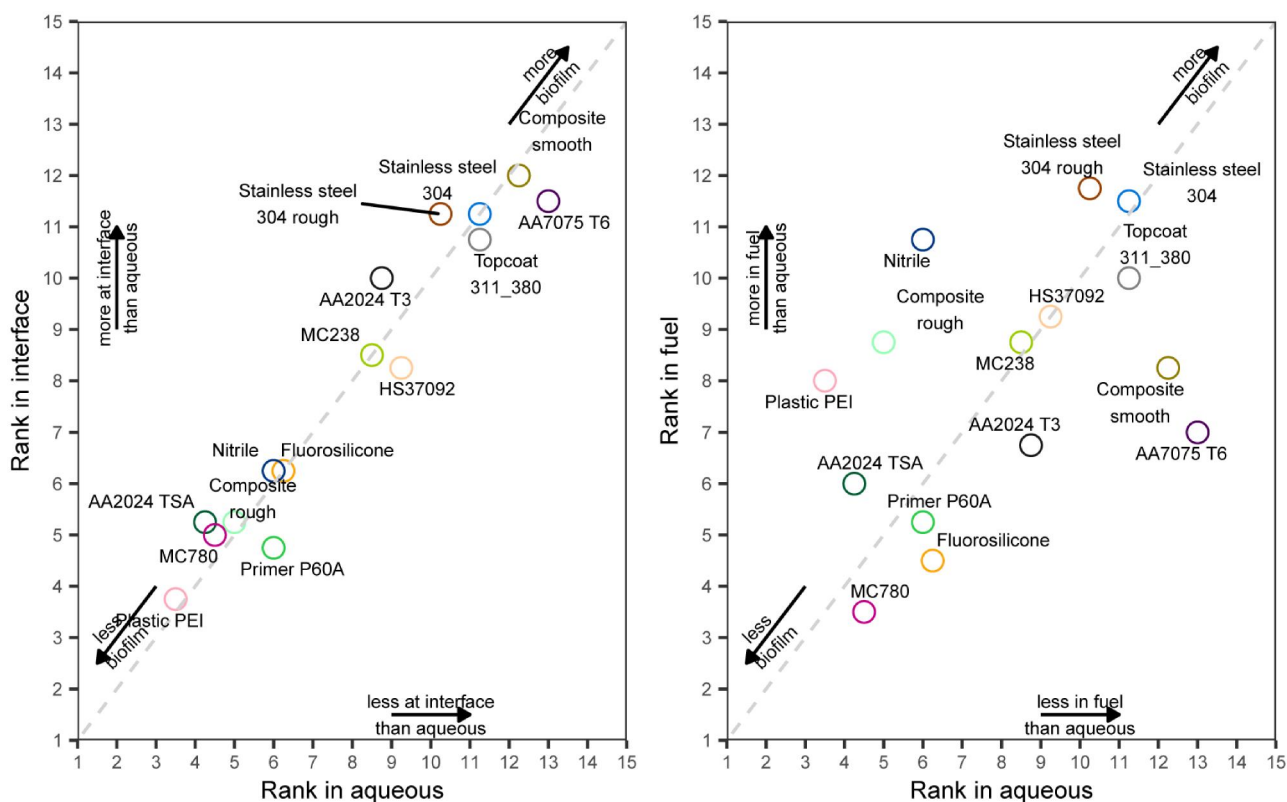


Figure 3. Biofilm coverage in the aqueous phase compared to biofilm coverage at (a) the fuel–water interface or (b) the fuel phase. Coverage on each material was ranked for *P. putida*, *R. erythropolis*, *C. tropicalis* and *A. resiniae* for each phase and the mean rank calculated. The grey line is a 1:1 relationship between rankings.

Table 2. Surface properties of materials.

Material	Roughness		Hydrophobicity Contact angle Degrees	Surface charge	
	Arithmetic mean height (Sa) (nm)			pH _{zpc}	At microcosm pH σ
	29 × 21 μm	634 × 476 μm			
AA7075 T6	198 ± 19.7	391 ± 31.2	67.6 ± 4.3	7.02	2.5
AA2024 T3	274.7 ± 49.7	473 ± 20.6	68.8 ± 5.4	6.63	−141.0
AA2024 TSA	569.7 ± 20.7	474 ± 31.3	82.5 ± 2.1	6.65	−76.6
SS304	74.4 ± 12.8	98.7 ± 2.8	60.2 ± 0.9	7.03	0.5
SS304 rough	154.4 ± 32.2	208.3 ± 5.4	60.4 ± 0.9	6.50	−36.0
Primer P60A	408 ± 32	1851.5 ± 2.5	90.1 ± 4.7	6.70	−74.0
Primer hs_37092	399.7 ± 16.2	1104.7 ± 31.7	64.6 ± 3.6	5.77	−338.6
Topcoat 311_380	17.9 ± 0.9	126.1 ± 25	55.6 ± 0.8	6.50	−47.1
Composite rough	nd	nd	52.3 ± 3.5	5.80	−190.8
Composite smooth	179.3 ± 30.5	1887 ± 100.8	62.5 ± 0.7	6.01	−195.0
Sealant MC238	467.3 ± 56.2	1097.3 ± 139.4	66 ± 0.6	5.40	−192.7
Sealant MC780	310 ± 30.2	1501.3 ± 172.3	83.6 ± 1.9	6.50	−68.6
Elastomer nitrile	120 ± 8.9	235.7 ± 6.6	52.8 ± 5	6.22	−152.6
Elastomer fluorosilicone	128.7 ± 8.1	423 ± 15.7	100.8 ± 3	5.75	−122.0
Plastic PEI	nd	nd	52.6 ± 1.4	7.20	17.9

Results are means ± SE. nd, not determined.

zero point charge for each material and the surface charge at the pH of the microcosm.

The relationship between biofilm coverage of each organism and material surface properties are shown in Supplementary Figure 3. As these relationships were complex and not explained by a single material property, random forest analyses were used to deduce properties that were most important in determining the coverage of each isolate. These results are summarised

in Figure 4. Results are present as root mean square error (RMSE) after permutation (larger values show that the parameter has a greater impact on the model) and Accumulated Local Effect profiles (which show how the different variables contribute to the model).

For *P. putida* the models explained 83.3% and 85.6% of the variance in coverage in the aqueous and fuel phases, respectively. The same surface parameters were identified as important in both phases, as

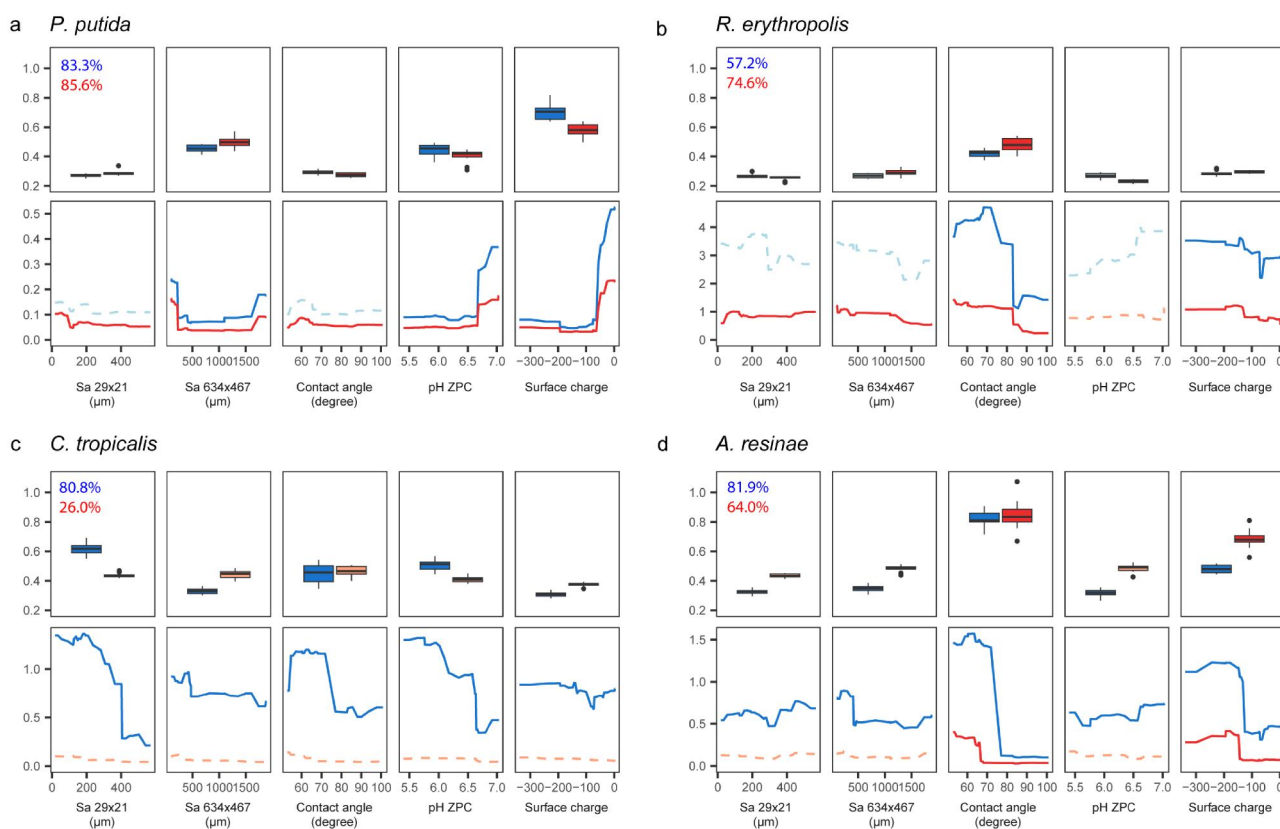


Figure 4. Random forest analysis of material surface properties and their influence on biofilm coverage. Separate analyses were performed for the aqueous (blue) and fuel (red) phases. The upper panel for each organism shows the reduction in root mean square error when values for that material are permuted. The numbers are the total variance explained by the model. The lower panel shows the Accumulated Local Effect profiles as % surface coverage. The data used for random forest analysis included an additional random term. Values that were greater than the random effect are shown as bold colours/solid lines. Values less than the random effect are shown as pale colours/dotted lines.

expected from the close correlation in biofilm coverage. Surface charge and pH of Zero Point Charge were the most important, with biofilm coverage favoured at surface charges close to zero, and pH ZPC close to neutral (Figure 4a). For *R. erythropolis*, the model only explained 57.2% of the variation in the aqueous phase, and 74.6% in the fuel phase. Contact angle was most important, with attachment favoured at contact angles less than 80° (i.e. hydrophilic surfaces) (Figure 4b). For *C. tropicalis* the model was uninformative in the fuel phase (explaining only 26% of the variation), reflecting the very limited biofilm growth in fuel. For the aqueous phase, surface roughness at the smaller scale, pH ZPC and contact angle all contributed, with biofilm formation favoured on smoother surfaces, with a pH ZPC of 6.5 or below, and contact angles less than 80° (Figure 4c). For *A. resiniae* contact angle and surface charge were important. Contact angles less than 80° in the aqueous phase and 70° in the fuel phase with surface charges less than $\sigma = -200$ favoured biofilm growth.

Overall, these analyses showed that different factors governed biofilm coverage for the four isolates tested. For example, *P. putida* biofilm formation was favoured on materials with surface charges close to 0 whereas *A. resiniae* biofilm formation was favoured when surface charges were $\sigma = -200$ or lower. Surface charge had limited influence on *R. erythropolis* or *C. tropicalis* biofilm formation. Where contact angle was found to be influential, attachment was favoured on hydrophilic surfaces.

Attachment of complex communities to surfaces

The analysis of individual isolates identified surfaces that were conducive to biofilm formation, those which restricted biofilm formation for some organisms and those that restricted biofilm formation for all organisms. To assess whether these results held true for diverse communities, selected materials were incubated in microcosms inoculated with a complex microbial community. Aluminium AA2024-T3, AA2024-T3-TSA

and AA7075-T6 were chosen as these metals showed significant variation in the attachment of the isolates. Nitrile and primer P60A were also tested as biofilm formation was low on these surfaces. Microcosms were inoculated with a complex community of microbes obtained originally from contaminated bottom water in an aircraft fuel tank. To select organisms that formed biofilms, coupons were removed from the microcosms every four weeks and placed into new microcosms containing sterile fuel and aqueous growth medium, simulating cycles of water removal and fuel consumption. The extent of biofilm formation was determined by quantification of extractable DNA, the absolute abundance of bacteria and fungi in these communities determined using qRT-PCR and community membership determined using high throughput sequencing of 16S rRNA and ITS genes.

The DNA yields from biofilm communities grown in the aqueous phase were much higher than the fuel phase (Figure 5a) ($p < 0.001$) but, in general, similar yields were obtained from different materials. qRT-PCR analysis showed that these complex communities contained more bacteria than fungi ($p < 0.001$) (Figure 5b). In the aqueous phase, the bacterial copy number was 10^4 – 10^5 copies μl^{-1} , but only 10^2 – 10^3 copies μl^{-1} in the fuel phase. There was little variation in 16S rRNA copy numbers between materials. The fungal ITS copy numbers were ~ 10 -fold lower, with lower numbers in the fuel phase compared to the aqueous phase. Again, values tended to be similar between the materials sampled, although lower on nitrile in the aqueous phase. Although the materials selected were based on differences in biofilm coverage of individual isolates, these differences were much less apparent when incubated with complex communities.

High throughput sequencing of 16S rRNA and ITS amplicons was used to explore the impact of material type and phase on community composition and complexity. Figure 5c and d show the mean relative abundance of bacterial and fungal Amplicon Sequence Variants (ASVs) in the biofilm communities. The starting inoculum was a complex, planktonic microbial community taken from the aqueous phase of a fuel:BH medium microcosm. It contained diverse bacteria (dominant genera included *Aquabacterium*, *Caulobacter*, *Pseudomonas*, *Rhodococcus*, *Sphingobium* and *Sphingopyxis* sp.) and fungi (largely *Candida keroseneae*, *Ascomycota* sp., *Metschnikowia* sp., *Plectosphaerella* and *A. resiniae*). These bacterial genera were present in both the fuel and aqueous phases of biofilm communities, although the relative proportion was influenced by the coupon material. The fungal

biofilm communities tended to differ more from the starting inoculum, with *Metschnikowia* sp. and *Plectosphaerella* more prevalent.

The diversity of bacterial communities on P60A and nitrile was lower than that on the aluminium surfaces (Supplementary Figure 4). For fungi, diversity indices were more variable, but were higher in the aqueous phase of AA2024 T3 and AA7075 than AA2024 TSA, nitrile or primer P60A. In the fuel phase, fungal diversity indices were similar, except for AA2024 TSA, which was lower.

The core microbiome for bacterial and fungal communities was identified by counting ASVs that were present in 2/3 of the samples at an abundance $> 0.1\%$. Figure 5e and f compares the core bacterial and fungal membership, comparing the starting inoculum with biofilm communities on all materials in the aqueous and fuel phase, and biofilm communities on different materials for the aqueous and fuel phases separately. The inoculum contained 74 bacterial and 26 fungal core members. A subset of these formed the core members of the biofilm communities on all materials. For bacteria, 44 were present in biofilms, 30 of which were common to both fuel and aqueous phases. The most common genera present in the core bacterial communities of both phases were *Rhodococcus* (12 members), *Caulobacter* and *Pseudomonas* (five members each). These genera were also the most common core members when different materials were compared: *Rhodococcus* (aqueous 12, fuel 13), *Pseudomonas* (aqueous 11, fuel 5) and *Caulobacter* (aqueous 5, fuel 5). Only six fungi were identified as core biofilm community members on all surfaces, of which four were common to both phases (one each of *Ascomycota* sp., *Candida keroseneae*, *Metschnikowia* and *Plectosphaerella*) – these were also common core members comparing different materials in the aqueous and fuel phases. Whilst core bacterial community members tended to be found on the majority of surfaces, fungi tended to be core members on a smaller subset of the materials, and sometimes only a single material.

The calculation of core community membership was based on presence/absence above a threshold value and did not account for changes in relative abundance. Therefore, an NMDS analysis (Figure 5g and h) and associated ANOVA (Table 3) of samples was performed using distances weighted for relative abundance (and phylogenetic relatedness for bacterial communities). For both the bacterial and fungal samples, there was a significant impact of both phase and material ($p < 0.001$). The bacterial communities growing on the different aluminium coupons were similar

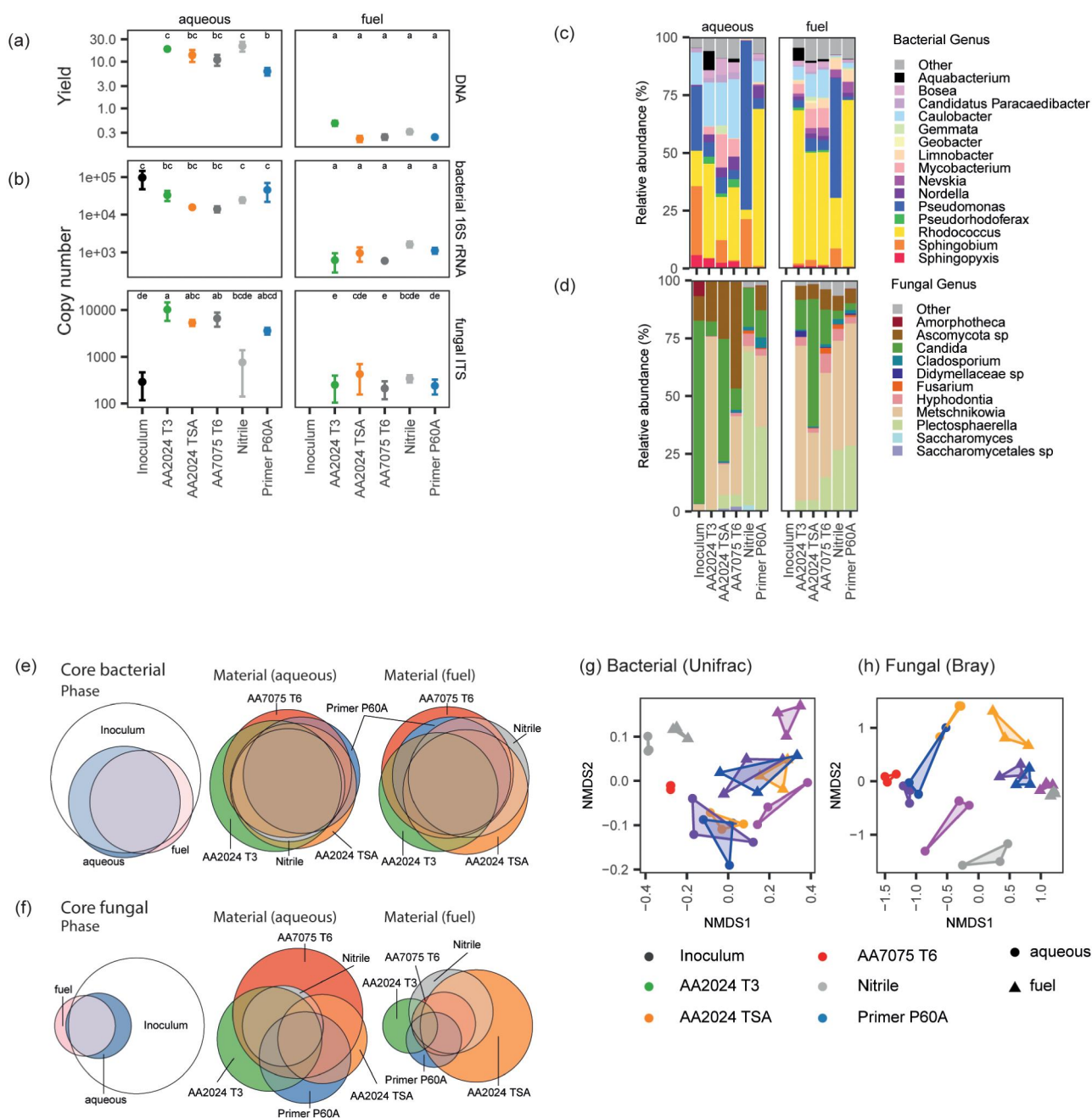


Figure 5. (a) DNA yields ($\text{ng } \mu\text{l}^{-1}$) (mean \pm SE) obtained from biofilms of complex communities in the aqueous or fuel phase grown on selected materials. Bacterial 16S and fungal ITS (b) copy numbers were determined by qRT-PCR. Samples with the same letters do not differ significantly from each other (log transformed data). The relative abundance of bacterial (c) and fungal (d) ITS regions at the genus level. Genera with a relative abundance $< 3\%$ in any sample are grouped as 'Other'. Euler diagrams of core bacterial (e) and fungal (f) community members comparing membership between phases on all materials or between materials in aqueous and fuel phases. Amplicon Sequence Variants (ASVs) were considered to be core if present in 2/3 of the samples at an abundance $> 0.1\%$. NMDS of samples using (g) the weighted Unifrac distance measure for bacteria and (h) weighted Bray distance measure for fungi. Each point represents a biological replicate.

while the fungal samples were distinct. For both bacterial and fungal samples, the communities growing on primer P60A and nitrile were distinct from those growing on aluminium surfaces.

Linear models implemented in DESeq2 were used to identify ASVs that differed significantly between

treatments. Comparisons were made between different materials in either the aqueous or fuel phase (Figure 6a and b) and between the aqueous and fuel phase for each material (Figure 6c and d). Comparisons between the fuel phase and aqueous phase for each material showed that the relative abundance of only a

Table 3. ANOVA analysis of the differences between bacterial and fungal communities on different materials.

Bacteria				
Material	AA2024 T3	AA2024 TSA	AA7075 T6	Primer P60A
AA2024 TSA	0.130			
AA7075 T6	0.279	0.352		
Primer P60A	0.004	0.005	0.014	
Nitrile	0.007	0.003	0.009	0.007
Fungi				
Material	AA2024 T3	AA2024 TSA	AA7075 T6	Primer P60A
AA2024 TSA	0.006			
AA7075 T6	0.013	0.005		
Primer P60A	0.005	0.008	0.006	
Nitrile	0.005	0.008	0.005	0.073

Results (*p* values) are shown for pairwise comparisons between materials.

small proportion of the bacterial community members was affected (>5%), with the exception of Primer P60A where 12% of the community differed (with *Pseudomonas*, *Caulobacter* and *Nordella* spp. favouring the aqueous phase). The impact of growth phase on the fungal community was greater on all materials (11–47% of the community differed) with *Plectosphaerella* and some *Metschnikowia* spp. favouring the fuel phase.

Comparisons between materials showed that the differences between communities growing on the aluminium surfaces was small in both phases. In most comparisons, less than 5% of the community differed between aluminium surfaces. The greatest impact was seen in comparisons between AA2024-T3 and AA2024-TSA where 10% of the bacterial community changed, the majority of which was due to a greater relative abundance of *Sphingobium* sp. on AA 2024 TSA and *Aquabacterium* sp. on AA2024 T3. For fungi, the relative abundance of *Metschnikowia* spp. was greater in the aqueous phase of AA2024 T3 compared to AA2024 TSA.

Greater differences were seen between the biofilm communities growing on the aluminium surfaces and those growing on Primer P60A and, particularly, nitrile. For bacteria the relative abundances of *Pseudomonads* and *Sphingobium* were much greater on nitrile in both the fuel and aqueous phases, whilst *Aquabacterium*, *Bosea*, *Candidatus Paracaedibacter*, *Caulobacter*, *Mycobacterium*, *Nordella*, *Pseudorhodofera* and *Rhodococcus* were greater on the aluminium surfaces. Inspection of ASVs favouring growth on nitrile showed that while the *Sphingobium* spp. always exhibited a preference for nitrile, individual *Pseudomonad* ASVs showed a preference either for nitrile (ASV11, ASV20, ASV4, ASV75, ASV8) or aluminium/primer surfaces (ASV131, ASV167, ASV192). Phylogenetic analysis showed that the ASVs that showed similar attachment behaviour clustered closely, with a clear distinction between those favouring nitrile or other surfaces (Figure 7).

For fungi, the relative abundance of *Hyphodontia*, *Plectosphaerella* and *Saccharomyces* genera were greater on nitrile in the aqueous phase, whilst *Ascomycota* sp. and *Metschnikowia* were greater on other surfaces. In the fuel phase, similar preferences were evident for *Ascomycota* sp. and *Metschnikowia*. *Candida keroseneae* favoured biofilm formation on nitrile in the aqueous phase, but aluminium surfaces in the fuel phase. Inspection showed that this was due to the different behaviour of two ASVs – in the fuel phase, fASV1 was a major component of AA7075 T6 and AA2024 TSA biofilm communities but was much reduced on nitrile. In contrast, in the aqueous phase, fASV22 favoured growth on nitrile, but was absent from the AA7075 T6 and AA2024 TSA biofilm communities.

Smaller differences were evident in comparisons with Primer P60A with *Caulobacter*, *Nordella* and *Rhodococcus* favouring Primer P60A when compared with nitrile and *Pseudomonas* favouring growth on nitrile compared with Primer P60A. *Aquabacterium*, *Mycobacterium*, *Pseudorhodofera* and *Sphingopyxis* favoured aluminium surfaces compared with Primer P60A in the aqueous phase.

Discussion

In this study, we examined biofilm formation on diverse surfaces with different surface properties found in aviation fuel systems. In aviation fuel tanks, water ingress leads to the formation of a fuel:aqueous interface; therefore, we examined biofilm formation in the aqueous, fuel and interface regions. With single microbial isolates, growth was favoured at the fuel:aqueous interface as this region provides the highest concentrations of nutrients within a hospitable aqueous environment (Passman 2003). Biofilm formation at the interface tended to correlate with formation in the aqueous phase across the isolates and materials tested, but this correlation was weaker when comparing the interface with the fuel phase, particularly for *R. erythropolis*.

R. erythropolis is a Gram-positive bacterium which is able to produce an extracellular matrix rich in hydrophobic lipids, modify their cell membrane fatty acid composition depending on the surface to which they are attached, and produce a diverse range of degradative enzymes (Rodrigues and de Carvalho 2015), all of which facilitate their attachment and growth on diverse surfaces in the fuel phase. This flexibility was likely responsible for *R. erythropolis* forming biofilms on most of the surfaces tested and

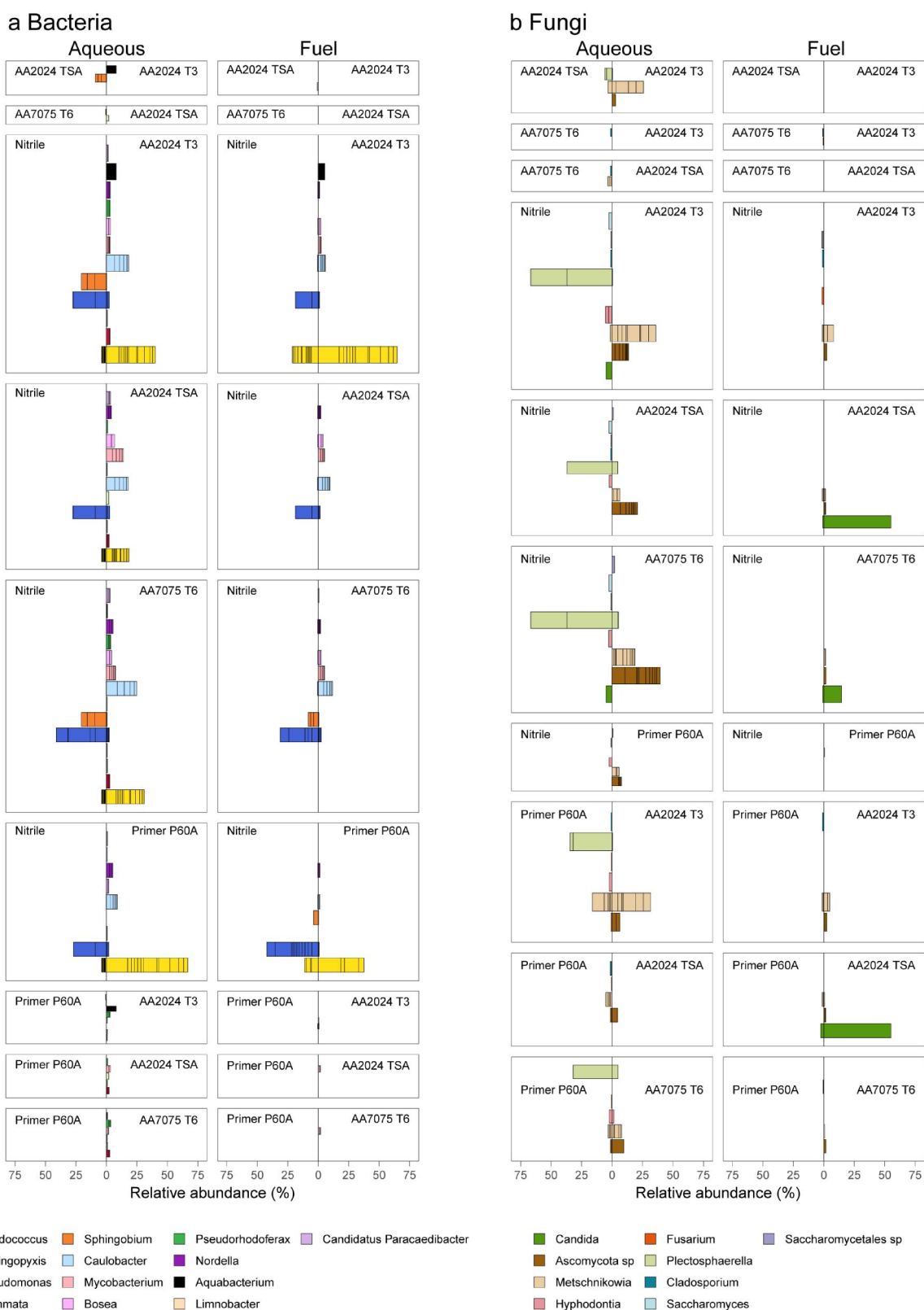


Figure 6. Comparisons of (a) bacterial and (b) fungal biofilm communities between the fuel and aqueous phases on different materials. Only ASVs that differed significantly between the materials are shown and have been coloured by genus. ASVs with a total relative abundance less than 0.5% have been omitted for clarity.

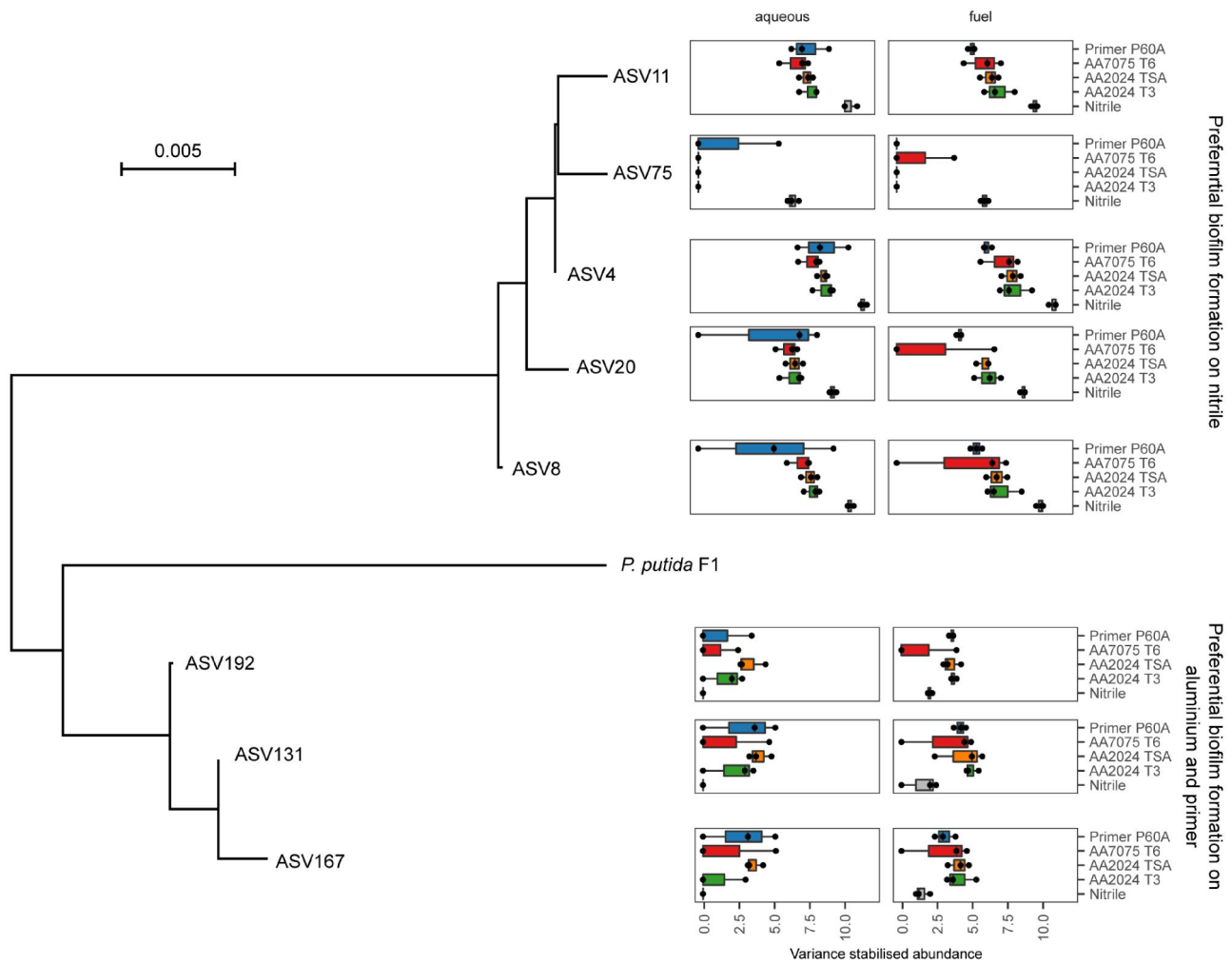


Figure 7. A phylogenetic tree constructed using the maximum likelihood method of *Pseudomonas* ASVs identified by high throughput sequencing that showed differential expression between materials and *P. putida* F1. The scale is the number of substitutions per site. Variance stabilised abundances from DESeq2 analysis for the materials in the aqueous and fuel biofilms are shown. Points are individual biological replicates. Boxplots are the median \pm interquartile ranges.

the inability to determine specific material surface properties related to coverage. For the other microbes tested, different surface properties influenced growth. For the *P. putida* isolate tested, biofilm coverage was favoured on surfaces with surface charge close to zero, a pH of ZPC close to neutral and smoother surfaces. Attachment is likely to be favoured under these conditions as the surface area for adhesion will be maximised and electrostatic repulsion of approaching microbes will be minimised (Carniello et al. 2018). However, as discussed below, in complex communities, other *Pseudomonas* strains behaved quite differently. In contrast, *A. resiniae* biofilm coverage was favoured on surfaces which were negatively charged, supporting the concept that no single set of surface material properties is likely to limit biofilm formation by diverse microbial communities.

The four isolates tested were representative of different microbial groups (Gram-positive and negative bacteria, yeasts and filamentous fungi) that are found as contaminants in fuel systems. We hypothesised that the behaviour of mixed microbial communities would be more complex. In an aircraft fuel tank, fuel is consumed and bottom water drained, removing most planktonic microbial cells. However, cells adhering to surfaces will be retained in the tank and receive a fresh influx of nutrients at regular intervals. We simulated this effect by transferring coupons between microcosms, thereby selecting microbial communities that could form biofilms on these materials. In addition, in complex communities, cells will be recruited to biofilms not only as a consequence of cell-surface interactions, but also cell-cell and cell-EPS interactions, thus increasing the diversity of biofilm

organisms. We selected three different aluminium materials, as these differed in their propensity for biofilm formation, then primer P60A and nitrile, as these tended to show limited biofilm formation with the single isolates. We recognise that there is considerable diversity in the complex microbial communities found in aviation fuel systems (Krohn et al. 2021) but the community used in the current study contains many of the organisms found in field samples.

Using DNA yield as a proxy for biomass accumulation, complex communities showed greater biofilm formation in the aqueous phase than the fuel phase, as was observed with individual isolates but, in contrast, there was little difference between the materials tested. Therefore, transferring coupons and the attached biofilms, at intervals into fresh fuel and media had selected for communities that were able to attach to similar extents. Quantitative PCR of the biofilm samples showed that the 16S rRNA copy numbers were ~10-fold higher than ITS copy numbers, indicating that the biofilm communities were dominated numerically by bacteria, although the relative abundance of eukaryotes in biofilms was much higher than that of the starting inoculum (with the exception of nitrile rubber). The ratio of bacteria to fungi observed in contaminated systems is variable and likely to be affected by 'founder' effects (i.e. the initial inoculum) and the physico-chemical environment, with acidic conditions favouring fungal growth (Krohn et al. 2021). For example, in contaminated diesel systems, Martin-Sanchez et al. (2018) found that bacteria were numerically dominant whilst Bückner et al. (2018) found similar systems were dominated by fungi.

Sequence analysis of the biofilm communities showed that they were diverse and contained at least 15 bacterial genera at relative abundances <3% including *Aquabacterium*, *Caulobacteria*, *Pseudomonas*, *Rhodococcus*, *Sphingobium* and *Sphingopyxis*, which have been reported as contaminants of fuel systems or present in fuel contaminated soils, able to degrade alkanes and form biofilms (Denaro et al. 2005, Garrido-Sanz et al. 2019, Itah et al. 2009, Kertesz and Kawasaki 2010, Masuda et al. 2014). The bacterial communities that developed on the different aluminium materials tested were similar, while those on nitrile and Primer P60A were distinct. However, these differences were caused, with the exception of nitrile, by relatively subtle shifts in the relative abundance of community members with only a small proportion (>10%) showing statistically significant differences between materials. This broad

similarity in bacterial populations was reflected in the core community composition which was largely shared between biofilms on different materials. The exception was nitrile, a highly hydrophobic surface, which became dominated by *Pseudomonads* and *Sphingobium* spp. with marked reductions in *Aquabacterium*, *Caulobacter* and *Rhodococcus* spp. The prevalence of *Pseudomonad* spp. on nitrile was initially surprising as *P. putida* F1 did not form significant biofilms on this material. However, this apparent contradiction was resolved when individual ASVs were analysed. Three genetically related *Pseudomonad* ASVs were identified that preferentially formed biofilms on materials other than nitrile, whilst four different, but genetically related, ASVs were identified as preferentially forming biofilms on nitrile compared to the Primer P60A and the three types of aluminium. The *Pseudomonads* are very diverse, metabolically flexible, are common in nature and can be found in both natural and constructed environments throughout the world (Ramos-Hegazy et al. 2021, Spiers et al. 2000), hence transferring material coupons had selected for a subset of the *Pseudomonad* community that was best able to attach. Similar observations were seen with pairs of closely related microbes that showed markedly different biofilm formation on a variety of artificial surfaces (Andrews et al. 2010). Nitrile rubber has been considered as a replacement material for incorporation into automatic taps used in medical facilities. Whilst initial differences in attachment were evident in *P. aeruginosa* biofilms, these did not translate into reduced cell numbers after 12 weeks incubation *in situ* in an experimental water distribution system, indicating that the flexibility of microbial metabolism counters attempts to select materials that limit biofilm formation (Hutchins et al. 2020).

Determination of the core fungal community showed that a much smaller proportion of the genera present in the initial inoculum became established in biofilms and that core community membership was more affected by the material. The initial inoculum was dominated by *A. resinae*, *Ascomycota* sp. and *Candida keroseneae*. However, in biofilms, *Metschnikowia* and *Plectosphaerella* spp. were also present at high relative abundances (these ASVs were detected at low abundance in the starting inoculum at low relative abundance). Although *Metschnikowia* and *Plectosphaerella* are not commonly reported as fuel degraders, *Metschnikowia* species have been described which can synthesise lipids from waste resources (Abeln et al. 2019, Santamauro et al. 2014) and *Plectosphaerella* spp.,

although typically described as plant pathogens, have been isolated from soil with the capability to degrade polyester polyurethane (Cosgrove et al. 2007). The biggest impact on the fungal biofilm community was again evident on nitrile, but there were also significant impacts on other materials. *Saccharomyces* spp. had a greater relative abundance on nitrile in the aqueous phase, with *Metschnikowia* and *Candida* spp. favouring the aluminium materials. Comparisons of biofilms between the fuel and aqueous phase showed that *Candida* spp. were most affected. Again, closer inspection of the sequence data showed that some *Candida* spp. favoured the fuel phase, whilst others favoured the aqueous phase.

Overall, this study has shown that biofilm coverage of individual isolates of typical fuel contaminant microbes is strongly influenced by material type, but that identifying materials, or material properties, which universally restrict biofilm formation is not possible. Materials such as nitrile, which tended to restrict biofilm formation with single isolates, were colonised by complex biofilm communities although the community structure was altered. Therefore, the introduction of different materials into aviation fuel systems will likely select for those organisms that are able to attach and it will be challenging to identify a set of material surface properties that limit all microbial growth. This selection effect was particularly evident with the pseudomonads, where studies with a single isolate (F1) identified a hierarchy of materials with respect to biofilm formation, whereas in complex communities, different *Pseudomonas* species were selected which were able to grow on different surfaces. Studies of individual isolates are essential to understanding the processes that allow microbes to attach to surfaces and form biofilms, but identifying approaches with the potential to limit biofilm formation or treat them with biocides in operational environments should consider the complexity of the diverse microbial communities that are found in aviation fuel systems.

Acknowledgements

This work was funded by Innovate UK Grant 113161 'Fuel Architecture Systems Technology (FAST)'. FAST is a collaborative Research & Technology project funded by ATI and the industrial partners.

Data sharing

The data that support the findings of this study are openly available in European Nucleotide Archive at <https://www.ebi.ac.uk/ena>, reference number PRJEB75686.

Disclosure statement

No potential conflict of interest was reported by the author(s).

Funding

This work was funded by Innovate UK Grant 113161 "Fuel Architecture Systems Technology (FAST)". FAST is a collaborative Research & Technology project funded by ATI and the industrial partners.

References

- Abarenkov K, Zirk A, Piirmann T, Pöhönen R, Ivanov F, Nilsson R, Kõljalg U. 2020. UNITE general FASTA release for Fungi. doi: [10.15156/bio/786368](https://doi.org/10.15156/bio/786368).
- Abeln F, Fan J, Budarin VL, Briers H, Parsons S, Allen MJ, Henk DA, Clark J, Chuck CJ. 2019. Lipid production through the single-step microwave hydrolysis of macroalgae using the oleaginous yeast *Metschnikowia pulcherrima*. *Algal Res.* 38:101411. doi: [10.1016/j.algal.2019.101411](https://doi.org/10.1016/j.algal.2019.101411).
- Andrews JS, Rolfe SA, Huang WE, Scholes JD, Banwart SA. 2010. Biofilm formation in environmental bacteria is influenced by different macromolecules depending on genus and species. *Environ Microbiol.* 12:2496–2507. doi: [10.1111/j.1462-2920.2010.02223.x](https://doi.org/10.1111/j.1462-2920.2010.02223.x).
- Banerjee I, Pangule RC, Kane RS. 2011. Antifouling coatings: recent developments in the design of surfaces that prevent fouling by proteins, bacteria, and marine organisms. *Adv Mater.* 23:690–718. doi: [10.1002/adma.201001215](https://doi.org/10.1002/adma.201001215).
- Berne C, Ellison CK, Ducret A, Brun YV. 2018. Bacterial adhesion at the single-cell level. *Nat Rev Microbiol.* 16: 616–627. doi: [10.1038/s41579-018-0057-5](https://doi.org/10.1038/s41579-018-0057-5).
- Bücker F, de Moura TM, da Cunha ME, de Quadros PD, Beker SA, Cazarolli JC, Caramão EB, Frazzon APG, Bento FM. 2018. Evaluation of the deteriogetic microbial community using qPCR, *n*-alkanes and FAMES biodegradation in diesel, biodiesel and blends (B5, B10, and B50) during storage. *Fuel.* 233:911–917. doi: [10.1016/j.fuel.2017.11.076](https://doi.org/10.1016/j.fuel.2017.11.076).
- Callahan BJ, McMurdie PJ, Rosen MJ, Han AW, Johnson AJA, Holmes SP. 2016. DADA2: high-resolution sample inference from Illumina amplicon data. *Nat Methods.* 13: 581–583. doi: [10.1038/nmeth.3869](https://doi.org/10.1038/nmeth.3869).
- Carniello V, Peterson BW, van der Mei HC, Busscher HJ. 2018. Physico-chemistry from initial bacterial adhesion to surface-programmed biofilm growth. *Adv Colloid Interface Sci.* 261:1–14. doi: [10.1016/j.cis.2018.10.005](https://doi.org/10.1016/j.cis.2018.10.005).
- Chan KY, Lam JKW. 2017. Water drop runoff in aircraft fuel tank vent systems. *Proc Inst Mech Eng Part C J Mech Eng Sci.* 231:4548–4563. doi: [10.1177/0954406216669175](https://doi.org/10.1177/0954406216669175).
- Cosgrove L, McGeechan PL, Robson GD, Handley PS. 2007. Fungal communities associated with degradation of polyester polyurethane in soil. *Appl Environ Microbiol.* 73:5817–5824. doi: [10.1128/AEM.01083-07](https://doi.org/10.1128/AEM.01083-07).
- Cribari-Neto F, Zeileis A. 2010. Beta regression in R. *J Stat Soft.* 34:1–24. doi: [10.18637/jss.v034.i02](https://doi.org/10.18637/jss.v034.i02).

- Denaro TR, Chelgren SK, Strobel EM, Balster LMT, Vangsness MD. 2005. DNA isolation of microbial contaminants in aviation turbine fuel via traditional polymerase chain reaction (PCR) and direct PCR. In: Airforce Research Laboratory: AFRL-PR-WP-TR-2006-2049; p. 1–17. <https://apps.dtic.mil/sti/tr/pdf/ADA446701.pdf>.
- Flemming H, Wingender J. 2010. The biofilm matrix. *Nat Rev Microbiol.* 8:623–633. doi: [10.1038/nrmicro2415](https://doi.org/10.1038/nrmicro2415).
- Garrido-Sanz D, Redondo-Nieto M, Guirado M, Pindado Jiménez O, Millán R, Martín M, Rivilla R. 2019. Metagenomic insights into the bacterial functions of a diesel-degrading consortium for the rhizoremediation of diesel-polluted soil. *Genes (Basel).* 10:456. doi: [10.3390/genes10060456](https://doi.org/10.3390/genes10060456).
- Gaylarde CC, Bento FM, Kelley J. 1999. Microbial contamination of stored hydrocarbon fuels and its control. *Rev Microbiol.* 30:01–10. doi: [10.1590/S0001-37141999000100001](https://doi.org/10.1590/S0001-37141999000100001).
- Gómez-Bolívar J, Warburton MP, Mumford AD, Mujica-Alarcón JF, Anguilano L, Onwukwe U, Barnes J, Chronopoulou M, Ju-Nam Y, Thornton SF, et al. 2024. Spectroscopic and microscopic characterization of microbial biofouling on aircraft fuel tanks. *Langmuir.* 40:3429–3439. doi: [10.1021/acs.langmuir.3c02803](https://doi.org/10.1021/acs.langmuir.3c02803).
- Gow NAR, Latge J-P, Munro CA. 2017. The fungal cell wall: structure, biosynthesis, and function. *Microbiol Spectr.* 5(3):1–25. doi: [10.1128/microbiolspec.FUNK-0035-2016](https://doi.org/10.1128/microbiolspec.FUNK-0035-2016).
- Hagenauer A, Hilpert R, Hack T. 1994. Microbiological investigations of corrosion damages in aircraft. *Mater Corros.* 45:355–360. doi: [10.1002/maco.19940450606](https://doi.org/10.1002/maco.19940450606).
- Hothorn T, Bretz F, Westfall P. 2008. Simultaneous inference in general parametric models. *Biom J.* 50:346–363. doi: [10.1002/bimj.200810425](https://doi.org/10.1002/bimj.200810425).
- Hu D, Zeng J, Wu S, Li X, Ye C, Lin W, Yu X. 2020. A survey of microbial contamination in aviation fuel from aircraft fuel tanks. *Folia Microbiol (Praha).* 65:371–380. doi: [10.1007/s12223-019-00744-w](https://doi.org/10.1007/s12223-019-00744-w).
- Hutchins CF, Moore G, Webb J, Walker JT. 2020. Investigating alternative materials to EPDM for automatic taps in the context of *Pseudomonas aeruginosa* and biofilm control. *J Hosp Infect.* 106:429–435. doi: [10.1016/j.jhin.2020.09.013](https://doi.org/10.1016/j.jhin.2020.09.013).
- Itah AY, Brooks AA, Ogar BO, Okure AB. 2009. Biodegradation of international jet A-1 aviation fuel by microorganisms isolated from aircraft tank and joint hydrant storage systems. *Bull Environ Contam Toxicol.* 83:318–327. doi: [10.1007/s00128-009-9770-0](https://doi.org/10.1007/s00128-009-9770-0).
- Kertesz MA, Kawasaki A. 2010. Hydrocarbon-degrading Sphingomonads: Sphingomonas, Sphingobium, Novosphingobium, and Sphingopyxis. In: Timmis KN, editor. *Handbook of hydrocarbon and lipid microbiology*. Berlin, Heidelberg: Springer Berlin Heidelberg; p. 1693–1705. doi: [10.1007/978-3-540-77587-4_119](https://doi.org/10.1007/978-3-540-77587-4_119).
- Klindworth A, Pruesse E, Schweer T, Peplies J, Quast C, Horn M, Glöckner FO. 2013. Evaluation of general 16S ribosomal RNA gene PCR primers for classical and next-generation sequencing-based diversity studies. *Nucleic Acids Res.* 41:e1. doi: [10.1093/nar/gks808](https://doi.org/10.1093/nar/gks808).
- Krohn I, Bergmann L, Qi M, Indenbirken D, Han Y, Perez-García P, Katzowitsch E, Hägele B, Lübcke T, Siry C, et al. 2021. Deep (meta)genomics and (meta)transcriptome analyses of fungal and bacteria consortia from aircraft tanks and kerosene identify key genes in fuel and tank corrosion. *Front Microbiol.* 12. doi: [10.3389/fmicb.2021.722259](https://doi.org/10.3389/fmicb.2021.722259).
- Kumar S, Stecher G, Li M, Knyaz C, Tamura K. 2018. MEGA X: molecular evolutionary genetics analysis across computing platforms. *Mol Biol Evol.* 35:1547–1549. doi: [10.1093/molbev/msy096](https://doi.org/10.1093/molbev/msy096).
- Lenth R. (2025). emmeans: Estimated marginal means, aka least-squares means. R package version 1.10.7. doi: [10.32614/CRAN.package.emmeans](https://doi.org/10.32614/CRAN.package.emmeans).
- Liaw A, Wiener M. 2002. Classification and regression by randomForest. *R News.* 2/3:18–22. <https://journal.r-project.org/articles/RN-2002-022/RN-2002-022.pdf>.
- Love MI, Huber W, Anders S. 2014. Moderated estimation of fold change and dispersion for RNA-seq data with DESeq2. *Genome Biol.* 15:550. doi: [10.1186/s13059-014-0550-8](https://doi.org/10.1186/s13059-014-0550-8).
- Martin-Sanchez PM, Gorbushina AA, Toepel J. 2018. Quantification of microbial load in diesel storage tanks using culture- and qPCR-based approaches. *Int Biodeterior Biodegradation.* 126:216–223. doi: [10.1016/j.ibiod.2016.04.009](https://doi.org/10.1016/j.ibiod.2016.04.009).
- Masuda H, Shiwa Y, Yoshikawa H, Zylstra GJ. 2014. Draft genome sequence of the versatile alkane-degrading bacterium *Aquabacterium* sp. strain NJ1. *Genome Announc.* 2(6):e01271-14. doi: [10.1128/genomeA.01271-14](https://doi.org/10.1128/genomeA.01271-14).
- McNamara CJ, Perry TD, Leard R, Bearce K, Dante J, Mitchell R. 2005. Corrosion of aluminum alloy 2024 by microorganisms isolated from aircraft fuel tanks. *Biofouling.* 21:257–265. doi: [10.1080/08927010500389921](https://doi.org/10.1080/08927010500389921).
- Meckenstock RU, von Netzer F, Stumpp C, Lueders T, Himmelberg AM, Hertkorn N, Schmitt-Kopplin P, Harir M, Hosein R, Haque S, et al. 2014. Water droplets in oil are microhabitats for microbial life. *Science.* 345:673–676. doi: [10.1126/science.1252215](https://doi.org/10.1126/science.1252215).
- Vejar ND, Paez M, Orrego A, Sancy M, Maria OT. 2017. Microbiologically influenced corrosion in aluminium alloys 7075 and 2024. In: *Aluminium alloys - recent trends in processing, characterization, mechanical behavior and applications*. Rijeka: IntechOpen. doi: [10.5772/intechopen.70735](https://doi.org/10.5772/intechopen.70735).
- Passman F. 2013. Microbial contamination and its control in fuels and fuel systems since 1980 – a review. *Int Biodeterior Biodegradation.* 81:88–104. doi: [10.1016/j.ibiod.2012.08.002](https://doi.org/10.1016/j.ibiod.2012.08.002).
- Passman FJ. 2003. Introduction to fuel microbiology. In: Passman F, editor. *Fuel and fuel system microbiology: fundamentals, diagnosis and contamination control*. West Conshohocken: ASTM International; p. 1–13. doi: [10.1520/MNL10443M](https://doi.org/10.1520/MNL10443M).
- R Core Team. 2021. R: a language and environment for statistical computing. Vienna, Austria: R Foundation for Statistical Computing.
- Rajasekar A, Ting Y-P. 2010. Microbial corrosion of aluminum 2024 aeronautical alloy by hydrocarbon degrading bacteria *Bacillus cereus* ACE4 and *Serratia marcescens* ACE2. *Ind Eng Chem Res.* 49:6054–6061. doi: [10.1021/ie100078u](https://doi.org/10.1021/ie100078u).
- Ramos-Hegazy L, Chakravarty S, Anderson G. 2021. The genus *Pseudomonas*. In: Green LH, Goldman E, editors.

- Practical handbook of microbiology. Boca Raton, FL: CRC Press. doi: [10.1201/9781003099277](https://doi.org/10.1201/9781003099277).
- Rauch ME, Graef HW, Rozenzhak SM, Jones SE, Bleckmann CA, Kruger RL, Naik RR, Stone MO. 2006. Characterization of microbial contamination in United States Air Force aviation fuel tanks. *J Ind Microbiol Biotechnol*. 33:29–36. doi: [10.1007/s10295-005-0023-x](https://doi.org/10.1007/s10295-005-0023-x).
- Renner LD, Weibel DB. 2011. Physicochemical regulation of biofilm formation. *MRS Bull*. 36:347–355. doi: [10.1557/mrs.2011.65](https://doi.org/10.1557/mrs.2011.65).
- Rodrigues CJ, de Carvalho CC. 2015. *Rhodococcus erythropolis* cells adapt their fatty acid composition during biofilm formation on metallic and non-metallic surfaces. *FEMS Microbiol Ecol*. 91:fiv135. doi: [10.1093/femsec/fiv135](https://doi.org/10.1093/femsec/fiv135).
- Santamauro F, Whiffin FM, Scott RJ, Chuck CJ. 2014. Low-cost lipid production by an oleaginous yeast cultured in non-sterile conditions using model waste resources. *Biotechnol Biofuels*. 7:34. doi: [10.1186/1754-6834-7-34](https://doi.org/10.1186/1754-6834-7-34).
- Schindelin J, Arganda-Carreras I, Frise E, Kaynig V, Longair M, Pietzsch T, Preibisch S, Rueden C, Saalfeld S, Schmid B, et al. 2012. Fiji: an open-source platform for biological-image analysis. *Nat Methods*. 9:676–682. doi: [10.1038/nmeth.2019](https://doi.org/10.1038/nmeth.2019).
- Schliep K, Potts AJ, Morrison DA, Grimm GW. 2017. Intertwining phylogenetic trees and networks. *Methods Ecol Evol*. 8:1212–1220. doi: [10.1111/2041-210X.12760](https://doi.org/10.1111/2041-210X.12760).
- Shapiro T, Chekanov K, Alexandrova A, Dolnikova G, Ivanova E, Lobakova E. 2021. Revealing of non-cultivable bacteria associated with the mycelium of fungi in the kerosene-degrading community isolated from the contaminated jet fuel. *J Fungi (Basel)*. 7:43. doi: [10.3390/jof7010043](https://doi.org/10.3390/jof7010043).
- Silhavy TJ, Kahne D, Walker S. 2010. The bacterial cell envelope. *Cold Spring Harb Perspect Biol*. 2:a000414. doi: [10.1101/cshperspect.a000414](https://doi.org/10.1101/cshperspect.a000414).
- Smith RN. 1991. Biodeterioration of fuels. In: Betts WB, editor. *Biodegradation: natural and synthetic materials*. London: Springer London; p. 55–68. doi: [10.1007/978-1-4471-3470-1_3](https://doi.org/10.1007/978-1-4471-3470-1_3).
- Song F, Koo H, Ren D. 2015. Effects of material properties on bacterial adhesion and biofilm formation. *J Dent Res*. 94:1027–1034. doi: [10.1177/0022034515587690](https://doi.org/10.1177/0022034515587690).
- Spiers AJ, Buckling A, Rainey PB. 2000. The causes of *Pseudomonas* diversity. *Microbiology (Reading)*. 146 (Pt 10):2345–2350. doi: [10.1099/00221287-146-10-2345](https://doi.org/10.1099/00221287-146-10-2345).
- Tamura K, Nei M. 1993. Estimation of the number of nucleotide substitutions in the control region of mitochondrial DNA in humans and chimpanzees. *Mol Biol Evol*. 10:512–526. doi: [10.1093/oxfordjournals.molbev.a040023](https://doi.org/10.1093/oxfordjournals.molbev.a040023).
- Turner B, Fein J. 2006. Protfit: a program for determining surface protonation constants from titration data. *Comput Geosci*. 32:1344–1356. doi: [10.1016/j.cageo.2005.12.005](https://doi.org/10.1016/j.cageo.2005.12.005).
- White J, Gilbert J, Hill G, Hill E, Huse SM, Weightman AJ, Mahenthalingam E. 2011. Culture-independent analysis of bacterial fuel contamination provides insight into the level of concordance with the standard industry practice of aerobic cultivation. *Appl Environ Microbiol*. 77:4527–4538. doi: [10.1128/aem.02317-10](https://doi.org/10.1128/aem.02317-10).
- White T, Bruns T, Lee S, Taylor J, Innis M, Gelfand D, Sninsky J. 1990. Amplification and direct sequencing of fungal ribosomal RNA genes for phylogenetics. In: Innis MA, Gelfand DH, Sninsky JJ, editors. *PCR protocols*. Academic Press Inc; p. 315–322. doi: [10.1016/B978-0-12-372180-8.50042-1](https://doi.org/10.1016/B978-0-12-372180-8.50042-1).